EUROPEAN ORGANIZATION FOR NUCLEAR RESEARCH

CERN-EP/89-170
20 December 1989

A High Statistics Measurement of the Deuteron Structure Functions $F_2(x,Q^2)$ and R from Deep Inelastic Muon Scattering at High Q^2

BCDMS Collaboration

A.C. Benvenuti, D. Bollini, G. Bruni and F.L. Navarria
Dipartimento di Fisica dell'Università and INFN, Bologna, Italy

A. Argento[1], W. Lohmann[2], L. Piemontese[3], J. Strachota[4] and P. Zavada[4]
CERN, Geneva, Switzerland

S. Baranov, V.I. Genchev[5], I.A. Golutvin, Yu.T. Kiryushin, V.G. Krivokhizhin, V.V. Kukhtin, R. Lednicky, S. Nemecek, P. Reimer[4], I.A. Savin, E. Telyukov, G.I. Smirnov, G. Sultanov[5], P. Todorov[5] and A.G. Volodko
Joint Institute for Nuclear Research, Dubna, USSR

D. Jamnik[6], R. Kopp[7], U. Meyer-Berkhout, A. Staude, K.-M. Teichert, R. Tirler[8], R. Voss[9] and C. Zupancic
Sektion Physik der Universität, München, Federal Republic of Germany[10]

M. Cribier, J. Feltesse, A. Milsztajn, A. Ouraou, Y. Sacquin, G. Smadja and M. Virchaux
DPhPE, CEN Saclay, France

Abstract

We present results on a high statistics study of the nucleon structure functions $F_2(x,Q^2)$ and $R=\sigma_L/\sigma_T$ measured in deep inelastic scattering of muons on a deuterium target. The analysis is based on $8\cdot10^5$ events after all cuts, recorded at beam energies of 120, 200 and 280 GeV in the kinematic range $0.06 \leq x \leq 0.80$ and $8\ \mathrm{GeV}^2 \leq Q^2 \leq 260\ \mathrm{GeV}^2$. Scaling violations observed in the data are in agreement with predictions of perturbative QCD and allow to determine the QCD mass scale parameter Λ.

Submitted to Physics Letters B

---

[1] Now at Digital Equipment, Torino, Italy.
[2] On leave from the Institut für Hochenergiephysik der AdW der DDR, Berlin-Zeuthen, GDR.
[3] Now at INFN, Ferrara, Italy.
[4] On leave from Institute of Physics, CSAV, Prague, Czechoslovakia.
[5] Now at the Institute of Nuclear Research and Nuclear Energy, Bulgarian Academy of Sciences, Sofia, Bulgaria.
[6] On leave from E. Kardelj University and the J. Stefan Institute, Ljubljana, Yugoslavia.
[7] Now at Siemens AG, Munich, Germany.
[8] Now at DPhPE, CEN Saclay, France.
[9] Now at CERN, Geneva, Switzerland.
[10] Funded in part by the German Federal Minister for Research and Technology (BMFT) under contract number 054MU12P6.

We present results on the structure functions of the nucleon measured with high statistics in deep inelastic scattering of muons on a deuterium target. In the one-photon exchange approximation, the deep inelastic muon-nucleon cross section can be written as

$$\frac{d^2\sigma}{dQ^2dx} = \frac{4\pi\alpha^2}{Q^4x}\left[1-y-\frac{Q^2}{4E^2}+\frac{y^2E^2+Q^2}{2E^2[R(x,Q^2)+1]}\right]F_2(x,Q^2) \qquad (1)$$

where E is the energy of the incident muon, Q^2 the squared four-momentum transfer between the muon and the nucleon, and x and y are the Bjorken scaling variables. This cross section depends on two structure functions F_2 and R, where $R=\sigma_L/\sigma_T$ is the ratio of absorption cross sections for virtual photons of longitudinal and transverse polarization.

The measurement which we describe here is similar to an earlier one with a hydrogen target [1,2,3]. The data were collected at the CERN SPS muon beam with a high-luminosity spectrometer which is described in detail elsewhere [4]. The results presented here are based on $8\cdot10^5$ reconstructed events after all cuts, recorded with positive muon beams of 120, 200 and 280 GeV energy. The kinematic ranges and data samples are summarized in Table 1. A part of these data has been used earlier in a study of nuclear effects [5]. The analysis of the data proceeds in exactly the same way as for the measurement with the hydrogen target and is also very similar to the analysis of our earlier carbon target data [6,7,8]. We therefore do not describe it here. Radiative corrections were calculated following ref. [9]. In comparison to the hydrogen data, the only additional contribution is due to coherent scattering on the deuteron.

The experimental results for R are given in Table 2 and are shown in Fig. 1 together with a perturbative QCD prediction R_{QCD} which is calculated from

$$R(x,Q^2) = \frac{F_L(x,Q^2) + \frac{4M^2x^2}{Q^2}F_2(x,Q^2)}{F_2(x,Q^2) - F_L(x,Q^2)} \qquad (2)$$

---

[1] In refs. [1] and [6], we have used a relation between R and F_L which is not consistent with the expression for F_L of eq. (3). This increases slightly the QCD prediction for R but does not affect the measured values. Since we used the perturbative QCD prediction for F_L in the computation of F_2, the latter decreases by approximately 1‰ over the entire kinematic range

where F_L is the longitudinal structure function and M is the mass of the nucleon.[1] In perturbative QCD, F_L is given by

$$F_L(x,Q^2) = \frac{\alpha_s(Q^2)}{2\pi} x^2 \int_x^1 \left[\frac{8}{3} F_2(z,Q^2) + \frac{40}{9}\left(1-\frac{x}{z}\right) z G(z,Q^2) \right] \frac{dz}{z^3} \qquad (3)$$

(ref. [10]) where $\alpha_s(Q^2)$ is the running coupling constant of QCD. To compute F_L, we assume a QCD mass scale parameter Λ = 220 MeV and a gluon momentum distribution $xG(x,Q_0^2) = 4.5(1-x)^8$ at Q_0^2 = 5 GeV^2 [2]. In the kinematic range of our data, R_{QCD} does not depend strongly on the gluon distribution assumed. The data lie above this prediction but there is no disagreement within the errors.

R_{QCD} was used to compute the structure function $F_2(x,Q^2)$ which is shown in Fig. 2 and is given in Tables 4 – 6 for the three different beam energies. The principal sources of systematic errors in the data are uncertainties in:

- the calibration of the incident beam energy ($\Delta E/E$ < 0.15%),
- the calibration of the spectrometer magnetic field B ($\Delta B/B$ < 0.15%),
- corrections for the energy loss ε of muons in iron [11] ($\Delta\varepsilon/\varepsilon$ < 1%),
- corrections for the finite resolution Σ of the spectrometer ($\Delta\Sigma/\Sigma$ < 5%),
- the relative cross section normalization of data taken at different beam energies (1% between the 120 GeV and 200 GeV data, 1.5% between the 280 GeV and 200 GeV data),
- the absolute cross section normalization (3%).

Most of the results presented in this paper, especially those on R and on the comparison of scaling violations to QCD predictions, are affected by the uncertainty on the relative but not on the absolute cross section normalization. Systematic errors originating from uncertainties in the detector efficiencies (0.5%) are small due to the redundancy in the experimental apparatus. The agreement between the different data sets in the region of large x confirms our estimate of most of the systematic errors as we have discussed in more detail in ref. [6].

---

of the data. This is completely negligible when compared to the errors.

The final $F_2(x,Q^2)$ from the combined data sets is shown in Fig. 3. Shown in the same figure are earlier EMC data from muon-deuterium scattering [12]. In comparison to these data we find a poor agreement, especially at small x, which is similar to the one observed in the hydrogen data [1]. Also shown in this figure are results from a recent analysis of SLAC data on electron-deuterium scattering at lower Q^2 [13]. In the region of $x \leq 0.35$ where the experiments cover disjoint ranges of Q^2, the SLAC data extrapolate to our results within the errors. At larger x and in the Q^2 region of overlap the errors of our data are dominated by the systematic uncertainties, which are strongly correlated. Within these errors, both data sets are compatible with a smooth Q^2 evolution of a common F_2.

Clear deviations from Bjorken scaling are observed in the structure function F_2 (Fig. 2). We compare these scaling violations to predictions of QCD using the same methods which we have applied previously to our carbon [7,8] and hydrogen [2,3] data. In the framework of perturbative QCD [18] scaling violations are due to the Q^2 evolution of quark and gluon distributions and can be described by the Altarelli-Parisi equations [19] or, alternatively, by the Q^2 dependence of their moments [20]. The data extend up to $x = 0.75$, thus requiring only little extrapolation to calculate the evolution integrals. Higher twist contributions to F_2, which are not described by these equations, vary like power series in $1/Q^2$ [21] and are expected to be small over most of the Q^2 range of our data.

Several numerical methods have been proposed to fit the QCD predictions to experimental data. We have mainly employed two methods [3,8,22] which have been developed within our collaboration. They allow to fit the flavour singlet and nonsinglet evolution equations both in a leading order (LO) perturbation expansion and in a next-to-leading order expansion in the $\overline{MS}$ renormalization scheme. Four quark flavours were assumed throughout the QCD analysis.

The experimental data shown in Fig. 2 were used for the fits. Data points with $y < 0.20$ at $x = 0.75$, $y < 0.16$ at $x = 0.65$ and $y < 0.14$ in all other bins of x were excluded to reduce the sensitivity of the fits to systematic uncertainties. Points with $Q^2 < 14$ GeV^2 at $0.16 < x < 0.25$ and with $Q^2 < 20$ GeV^2 at $x > 0.25$ were excluded to suppress possible higher twist effects. These cuts are the same as in the analysis of the hydrogen data.

In the nonsinglet approximation, the gluon contribution is neglected in the evolution equations. Estimates of the gluon distribution from muon [2,7,14,15] and neutrino scattering experiments [16,17] have shown that this approximation is valid at high values of x. Therefore, in the nonsinglet analysis of the data reported here, only the kinematic region $x \geq 0.275$ was used. The cut at $Q^2 = 20$ GeV^2 further reduces the contribution of the gluon distribution which becomes softer with increasing Q^2 due to its QCD evolution. The results of these fits are summarized in Table 3. We find good agreement between the values of Λ obtained with the different programs. The average result for the QCD mass scale parameter in next-to-leading order is

$$\Lambda_{\overline{MS}} = 230 \pm 40\,(stat.) \pm 70\,(syst.)\,MeV,$$

corresponding to a strong coupling constant of

$$\alpha_S(Q^2 = 100\ GeV^2) = 0.160 \pm 0.006\,(stat.) \pm 0.011\,(syst.).$$

This is in good agreement with the result of our earlier measurements on carbon and hydrogen targets, $\Lambda_{\overline{MS}} = 220 \pm 15\,(stat.) \pm 50\,(syst.)$ MeV [2,7]. To evaluate the systematic errors on Λ and α_S, the individual systematic uncertainties on F_2 were added to the data and the fits repeated. This was done for each contribution to the systematic error in turn and the resulting changes in Λ were combined in quadrature. The final systematic error $\Delta\Lambda = 70$ MeV is dominated by the uncertainty on the relative normalization between data taken at the three different beam energies.

As we have discussed in more detail in refs. [2,7], the agreement between data and QCD fit, which is prerequisite for a meaningful determination of α_S, is best verified by comparing the x dependence of measured and predicted scaling violations. This is shown for the nonsinglet case in Fig. 4a where the average logarithmic derivatives $d\ln F_2(x,Q^2)/d\ln Q^2$ are compared to the next-to-leading order prediction for $\Lambda_{\overline{MS}} = 230$ MeV. The measured x dependence of the scaling violations is in agreement with the predicted one.

In the QCD analysis over the full x range of the data, the Q^2 evolution of the deuteron structure function, which is an almost pure flavour singlet, is sensitive to the gluon distribution at small x. We

use the gluon distribution $xG(x) \propto (1-x)^8$ at $Q_0^2 = 5$ GeV^2 determined in next-to-leading order from our hydrogen data [2] and fit Λ over the full kinematic range of the data. This fit yields $\Lambda_{\overline{MS}} = 250 \pm 35$ (*stat.*) MeV in agreement with the result of the nonsinglet fit. The measured logarithmic derivatives and the corresponding QCD prediction for $\Lambda_{\overline{MS}} = 250$ MeV are shown in Fig. 4b. Treating the power of the gluon distribution as a free parameter in the fit gives compatible results within large errors.

In conclusion, we have presented a high statistics measurement of the deuteron structure functions F_2 and R from deep inelastic scattering of muons at high Q^2 on a deuterium target. Scaling violations are observed in the data and are in agreement with predictions from perturbative QCD. We find $\Lambda_{\overline{MS}}$ to be in good agreement with our earlier result obtained with carbon and hydrogen targets.

References

1. BCDMS, A.C. Benvenuti et al., Phys. Lett. 223B (1989) 485.
2. BCDMS, A.C. Benvenuti et al., Phys. Lett. 223B (1989) 490.
3. A. Ouraou, Thèse, Université Paris XI, 1988.
4. BCDMS, D. Bollini et al., Nucl. Instr. Meth. 204 (1983) 333;
   BCDMS, A.C. Benvenuti et al., Nucl. Instr. Meth. 226 (1984) 330.
5. BCDMS, G. Bari et al., Phys. Lett. 163B (1985) 282;
   BCDMS, A.C. Benvenuti et al., Phys. Lett. 189B (1987) 483;
   A. Milsztajn, Thèse Université Paris XI, 1989.
6. BCDMS, A.C. Benvenuti et al., Phys. Lett. 195B (1987) 91.
7. BCDMS, A.C. Benvenuti et al., Phys. Lett. 195B (1987) 97.
8. M. Virchaux, Thèse, Université Paris VII, 1988.
9. A.A. Akhundov et al., Sov. J. Nucl. Phys. 26 (1977) 660;
   D.Yu. Bardin and N.M. Shumeiko, Sov. J. Nucl. Phys. 29 (1979) 499;
   A.A. Akhundov et al., Sov. J. Nucl. Phys. 44 (1986) 988;
   A.A. Akhundov et al., JINR Communication E2-86-104, Dubna 1986.
10. G. Altarelli and G. Martinelli, Phys. Lett. 76B (1978) 89.
11. BCDMS, R. Kopp et al., Z. Phys. C28 (1985) 171;
    W. Lohmann, R. Kopp and R. Voss, CERN 85-03 (CERN Yellow Report).
12. EMC, J.J. Aubert et al., Nucl. Phys. B293 (1987) 740.
13. L.W. Whitlow et al., Univ. of Rochester Preprint UR-1119 (ER-13065-586), subm. to Europhysics Conf. on High Energy Physics, Madrid, Spain, 1989.
14. EMC, J.J. Aubert et al., Nucl. Phys. B259 (1985) 189.
15. EMC, J.J. Aubert et al., Nucl. Phys. B272 (1986) 158.
16. CDHS, H. Abramowicz et al., Z. Phys. C17 (1983) 283;
    CDHSW, P. Berge et al., CERN-EP/89-103, subm. to Zeitschrift für Physik C.

17. CHARM, F. Bergsma et al., Phys. Lett. 123B (1983) 269 and Phys. Lett. 153B (1985) 111.

18. For extensive reviews of perturbative QCD and further references, see:

A. Buras, Rev. Mod. Phys. 52 (1980) 199; G. Altarelli, Phys. Rep. 81 (1982) 1.

19. G. Altarelli and G. Parisi, Nucl. Phys. B126 (1977) 298.

20. For a review, see D.W. Duke and R.G. Roberts, Phys. Rep. 120 (1985) 275.

21. See e.g. R.K. Ellis, W. Furmanski and R. Petronzio, Nucl. Phys. B212 (1983) 29.

22. V.G. Krivokhizhin et al., Z. Physik C 36 (1987) 51.

Table Captions

Table 1: Kinematic ranges and number of events after all cuts at the three different beam energies.

Table 2: Results for $R=\sigma_L/\sigma_T$ as a function of x. R is averaged over Q^2 in each bin of x.

Table 3: Results of nonsinglet QCD fits to $F_2(x,Q^2)$ in leading order (LO) and next-to-leading order in the $\overline{MS}$ renormalisation scheme. The data are fitted in the kinematic range $x \geq 0.275$ and $Q^2 \geq 20$ GeV^2; additional cuts on y are discussed in the text. Four quark flavours are assumed in the QCD analysis. χ^2_S is the χ^2 of the direct comparison between measured and predicted scaling violations (Fig. 4a). Only statistical errors are given; systematic errors are discussed in the text.

Table 4: $F_2(x,Q^2)$ measured at 120 GeV beam energy. The average beam energy at the interaction vertex is $<E> = 117.6$ GeV. $F_2(x,Q^2)$ is given both for $R = \sigma_L/\sigma_T = 0$ (F_2^0) and for $R = R_{QCD}$ (F_2^{QCD}). The statistical error ΔF_2 applies to F_2^0 and can be scaled to apply to F_2^{QCD}. The systematic errors are given in form of factors f; the distorted F_2 is obtained either multiplying or dividing the given $F_2(x,Q^2)$ by these factors. We call f_b, f_s and f_r the uncertainties due to beam momentum calibration, spectrometer magnetic field calibration and spectrometer resolution, respectively; f_d is the systematic error due to detector and trigger inefficiencies and f_n due to the uncertainty in the relative normalization of data from external and internal targets. The overall normalization uncertainties discussed in the text are not given here.

Table 5: As Table 4, for the measurement at 200 GeV beam energy. The average beam energy at the interaction vertex is $<E> = 196.2$ GeV.

Table 6: As Table 4, for the measurement at 280 GeV beam energy. The average beam energy at the interaction vertex is $<E> = 275.8$ GeV.

Table 1: The data sample

Beam energy (GeV)	Q^2 range (GeV^2)	x range	Number of events
120	8-106	0.06-0.80	311 000
200	16-150	0.06-0.80	385 000
280	30-260	0.08-0.80	77 000

Table 2: Results for R

x	$<Q^2>$ (GeV^2)	R	ΔR (*stat.*)	ΔR (*syst.*)
0.10	20.0	0.190	0.120	0.072
0.14	25.0	0.114	0.076	0.046
0.18	35.0	0.160	0.077	0.038
0.225	45.0	0.222	0.069	0.041
0.275	50.0	0.061	0.049	0.036
0.35	65.0	0.077	0.042	0.034
0.45	75.0	0.060	0.062	0.036
0.55	85.0	0.165	0.120	0.056
0.65	85.0	0.043	0.181	0.107

Table 3: Results of nonsinglet QCD fits

Method	Λ_{LO} (MeV)	χ^2/DOF	χ^2_S/DOF	$\Lambda_{\overline{MS}}$ (MeV)	χ^2/DOF	χ^2_S/DOF
Ref. [3,8]	210±37	123/155	6.5/5	236±39	126/155	9.2/5
Ref. [22]	206±35	135/154	5.9/5	220±34	140/154	8.2/5

Table 4: $F_2(x,Q^2)$ at 120 GeV beam energy

x	Q^2 (GeV^2)	F_2^0	ΔF_2	F_2^{QCD}	f_b	f_s	f_r	f_d	f_n
0.07	8.75	0.36575	0.00643	0.38165	0.997	0.999	1.003	1.015	1.010
	10.25	0.36092	0.00606	0.38360	0.997	0.999	1.008	1.015	1.010
0.10	10.25	0.35360	0.00437	0.36055	0.996	0.998	1.005	1.005	1.010
	11.75	0.35702	0.00463	0.36655	0.996	0.999	1.006	1.005	1.010
	13.25	0.34834	0.00489	0.36055	0.997	0.999	1.004	1.005	1.010
0.14	11.75	0.33013	0.00504	0.33304	0.995	0.998	1.002	1.000	1.010
	13.25	0.34016	0.00544	0.34403	0.996	0.998	1.004	1.000	1.010
	15.00	0.33475	0.00498	0.33974	0.996	0.999	1.004	1.000	1.010
	17.00	0.33123	0.00554	0.33773	0.996	0.999	1.002	1.000	1.010
	19.00	0.33780	0.00632	0.34631	0.997	0.999	1.000	1.000	1.010
0.18	11.75	0.31451	0.00599	0.31578	0.995	0.997	0.998	1.000	1.010
	13.25	0.31298	0.00605	0.31458	0.995	0.998	1.000	1.000	1.010
	15.00	0.30061	0.00544	0.30259	0.996	0.998	1.002	1.000	1.010
	17.00	0.30601	0.00612	0.30863	0.996	0.999	1.003	1.000	1.010
	19.00	0.30947	0.00668	0.31282	0.996	0.999	1.003	1.000	1.010
	21.50	0.29547	0.00591	0.29966	0.997	0.999	1.002	1.000	1.010
	24.50	0.29306	0.00719	0.29859	0.997	1.000	1.000	1.000	1.010
0.225	11.75	0.27761	0.00562	0.27821	0.995	0.998	1.002	1.000	1.010
	13.25	0.28678	0.00594	0.28755	0.995	0.998	1.002	1.000	1.010
	15.00	0.27833	0.00535	0.27928	0.996	0.998	1.001	1.000	1.010
	17.00	0.27099	0.00560	0.27217	0.996	0.999	1.000	1.000	1.010
	19.00	0.27198	0.00615	0.27346	0.996	0.999	1.002	1.000	1.010
	21.50	0.26953	0.00556	0.27142	0.996	0.999	1.003	1.000	1.010
	24.50	0.26596	0.00621	0.26840	0.997	1.000	1.001	1.000	1.010
	28.00	0.25886	0.00557	0.26202	0.997	1.000	1.003	1.000	1.000
	32.50	0.25756	0.00547	0.26189	0.997	1.000	1.002	1.000	1.000
0.275	13.25	0.25851	0.00631	0.25894	0.996	0.999	1.003	1.000	1.010
	15.00	0.24795	0.00543	0.24846	0.996	1.000	1.007	1.000	1.010
	17.00	0.23909	0.00569	0.23970	0.996	1.000	1.002	1.000	1.010
	19.00	0.23758	0.00624	0.23833	0.996	1.000	1.005	1.000	1.010
	21.50	0.23279	0.00551	0.23372	0.997	1.000	1.000	1.000	1.010
	24.50	0.23450	0.00436	0.23571	0.997	1.000	1.003	1.000	1.004
	28.00	0.23381	0.00411	0.23538	0.997	1.001	0.998	1.000	1.004
	32.50	0.22833	0.00431	0.23041	0.997	1.001	1.001	1.000	1.002
	37.50	0.21961	0.00566	0.22231	0.997	1.001	1.004	1.000	1.000
	43.00	0.21705	0.00578	0.22061	0.997	1.001	1.007	1.000	1.000

Table 4: $F_2(x,Q^2)$ at 120 GeV beam energy (continued)

x	$Q^2\,(GeV^2)$	F_2^0	ΔF_2	F_2^{QCD}	f_b	f_s	f_r	f_d	f_n
0.35	13.25	0.18290	0.00423	0.18309	0.999	1.004	1.007	1.000	1.010
	15.00	0.18873	0.00387	0.18897	0.998	1.003	1.007	1.000	1.010
	17.00	0.17893	0.00398	0.17921	0.998	1.003	1.001	1.000	1.010
	19.00	0.17382	0.00416	0.17414	0.998	1.003	1.004	1.000	1.010
	21.50	0.18531	0.00393	0.18573	0.998	1.003	0.997	1.000	1.010
	24.50	0.17836	0.00288	0.17887	0.998	1.003	1.005	1.000	1.004
	28.00	0.17729	0.00268	0.17794	0.998	1.003	1.003	1.000	1.004
	32.50	0.17661	0.00275	0.17747	0.998	1.003	1.000	1.000	1.003
	37.50	0.17234	0.00372	0.17344	0.998	1.002	1.000	1.000	1.000
	43.00	0.16928	0.00364	0.17070	0.998	1.002	1.005	1.000	1.000
	49.50	0.16545	0.00377	0.16729	0.998	1.002	1.001	1.000	1.000
	57.00	0.16205	0.00431	0.16445	0.998	1.002	1.005	1.000	1.000
0.45	13.25	0.12068	0.00403	0.12077	1.007	1.015	1.003	1.000	1.010
	15.00	0.11853	0.00364	0.11864	1.006	1.014	0.997	1.000	1.010
	17.00	0.12108	0.00388	0.12121	1.004	1.012	0.995	1.000	1.010
	19.00	0.11283	0.00402	0.11297	1.003	1.011	1.008	1.000	1.010
	21.50	0.11759	0.00367	0.11777	1.003	1.010	1.002	1.000	1.010
	24.50	0.10949	0.00246	0.10969	1.002	1.009	1.000	1.000	1.004
	28.00	0.10915	0.00231	0.10940	1.001	1.008	1.003	1.000	1.004
	32.50	0.10904	0.00230	0.10935	1.000	1.007	0.999	1.000	1.003
	37.50	0.10842	0.00266	0.10882	1.000	1.007	0.999	1.000	1.002
	43.00	0.10518	0.00303	0.10567	0.999	1.006	1.005	1.000	1.000
	49.50	0.09777	0.00303	0.09836	0.999	1.005	1.004	1.000	1.000
	57.00	0.10295	0.00333	0.10376	0.998	1.005	1.008	1.000	1.000
	65.50	0.09701	0.00350	0.09801	0.998	1.005	1.002	1.000	1.000
	75.00	0.09586	0.00414	0.09714	0.998	1.004	1.000	1.000	1.000
0.55	15.00	0.05869	0.00241	0.05873	1.020	1.034	1.021	1.000	1.010
	17.00	0.05714	0.00256	0.05719	1.017	1.030	1.018	1.000	1.010
	19.00	0.06287	0.00303	0.06293	1.014	1.027	1.007	1.000	1.010
	21.50	0.05920	0.00264	0.05927	1.012	1.024	1.008	1.000	1.010
	24.50	0.05595	0.00280	0.05603	1.010	1.021	1.007	1.000	1.010
	28.00	0.05904	0.00172	0.05914	1.008	1.019	1.007	1.000	1.004
	32.50	0.05668	0.00171	0.05680	1.006	1.016	1.004	1.000	1.003
	37.50	0.05511	0.00194	0.05526	1.004	1.014	1.005	1.000	1.002
	43.00	0.05589	0.00234	0.05607	1.003	1.013	1.005	1.000	1.000
	49.50	0.05493	0.00241	0.05516	1.002	1.011	1.004	1.000	1.000
	57.00	0.04965	0.00240	0.04991	1.001	1.010	1.001	1.000	1.000
	65.50	0.05175	0.00270	0.05210	1.000	1.009	1.000	1.000	1.000
	75.00	0.04983	0.00286	0.05026	0.999	1.008	0.999	1.000	1.000
	86.00	0.04681	0.00298	0.04732	0.999	1.008	1.002	1.000	1.000

Table 4: $F_2(x,Q^2)$ at 120 GeV beam energy (continued)

x	$Q^2\ (GeV^2)$	F_2^0	ΔF_2	F_2^{QCD}	f_b	f_s	f_r	f_d	f_n
0.65	17.00	0.02807	0.00152	0.02809	1.040	1.063	1.086	1.000	1.010
	19.00	0.02869	0.00176	0.02872	1.035	1.056	1.073	1.000	1.010
	21.50	0.02673	0.00151	0.02676	1.030	1.050	1.068	1.000	1.010
	24.50	0.02861	0.00183	0.02864	1.025	1.044	1.057	1.000	1.010
	28.00	0.02370	0.00159	0.02373	1.021	1.039	1.047	1.000	1.010
	32.50	0.02460	0.00100	0.02464	1.017	1.034	1.034	1.000	1.003
	37.50	0.02521	0.00119	0.02526	1.014	1.029	1.027	1.000	1.002
	43.00	0.02659	0.00152	0.02666	1.011	1.026	1.022	1.000	1.000
	49.50	0.02449	0.00157	0.02457	1.008	1.023	1.018	1.000	1.000
	57.00	0.02296	0.00163	0.02305	1.006	1.020	1.013	1.000	1.000
	65.50	0.02062	0.00168	0.02072	1.004	1.018	1.012	1.000	1.000
	75.00	0.02491	0.00211	0.02507	1.003	1.016	1.010	1.000	1.000
	86.00	0.01926	0.00194	0.01941	1.001	1.014	1.011	1.000	1.000
	99.00	0.02329	0.00234	0.02352	1.000	1.013	1.007	1.000	1.000
0.75	32.50	0.00867	0.00054	0.00868	1.040	1.069	1.094	1.000	1.000
	37.50	0.00984	0.00073	0.00986	1.033	1.060	1.084	1.000	1.000
	43.00	0.00800	0.00070	0.00802	1.027	1.052	1.075	1.000	1.000
	49.50	0.00861	0.00082	0.00863	1.022	1.046	1.066	1.000	1.000
	57.00	0.00876	0.00092	0.00879	1.017	1.040	1.055	1.000	1.000
	65.50	0.00785	0.00098	0.00788	1.013	1.035	1.049	1.000	1.000
	75.00	0.00775	0.00110	0.00779	1.010	1.031	1.035	1.000	1.000
	86.00	0.00707	0.00115	0.00711	1.007	1.027	1.030	1.000	1.000
	99.00	0.00651	0.00123	0.00656	1.004	1.024	1.023	1.000	1.000

Table 5: $F_2(x,Q^2)$ at 200 GeV beam energy

x	$Q^2\,(GeV^2)$	F_2^0	ΔF_2	F_2^{QCD}	f_b	f_s	f_r	f_d	f_n
0.07	17.00	0.37420	0.00686	0.39517	0.997	0.999	0.996	1.015	1.005
	19.00	0.36040	0.00597	0.38663	0.997	1.000	1.005	1.015	1.005
0.10	19.00	0.35627	0.00466	0.36425	0.996	0.999	1.004	1.005	1.005
	21.50	0.36119	0.00392	0.37191	0.997	0.999	1.006	1.005	1.005
	24.50	0.35010	0.00416	0.36414	0.997	0.999	1.003	1.005	1.005
0.14	21.50	0.33493	0.00434	0.33812	0.996	0.998	1.005	1.000	1.005
	24.50	0.34013	0.00457	0.34444	0.996	0.999	1.007	1.000	1.005
	28.00	0.32720	0.00419	0.33278	0.996	0.999	1.003	1.000	1.005
	32.50	0.32015	0.00421	0.32780	0.997	1.000	1.004	1.000	1.005
0.18	21.50	0.30177	0.00485	0.30303	0.995	0.998	1.005	1.000	1.005
	24.50	0.30154	0.00493	0.30320	0.996	0.998	1.002	1.000	1.005
	28.00	0.30541	0.00465	0.30764	0.996	0.999	1.003	1.000	1.005
	32.50	0.30445	0.00369	0.30751	0.996	0.999	1.004	1.000	1.003
	37.50	0.29470	0.00376	0.29877	0.997	1.000	0.998	1.000	1.002
	43.00	0.29398	0.00373	0.29948	0.997	1.000	1.001	1.000	1.002
0.225	28.00	0.27552	0.00443	0.27651	0.996	0.999	0.997	1.000	1.005
	32.50	0.26457	0.00421	0.26586	0.996	0.999	1.002	1.000	1.005
	37.50	0.26632	0.00339	0.26808	0.996	1.000	0.999	1.000	1.002
	43.00	0.26452	0.00331	0.26686	0.997	1.000	1.003	1.000	1.002
	49.50	0.25623	0.00334	0.25931	0.997	1.000	1.005	1.000	1.002
	57.00	0.24538	0.00436	0.24941	0.997	1.001	1.003	1.000	1.000
0.275	28.00	0.24510	0.00457	0.24560	0.996	1.000	1.003	1.000	1.005
	32.50	0.23687	0.00433	0.23751	0.997	1.000	0.996	1.000	1.005
	37.50	0.22244	0.00325	0.22324	0.997	1.001	1.000	1.000	1.003
	43.00	0.22320	0.00321	0.22426	0.997	1.001	0.998	1.000	1.002
	49.50	0.22215	0.00327	0.22357	0.997	1.001	1.004	1.000	1.002
	57.00	0.21767	0.00344	0.21954	0.997	1.001	1.001	1.000	1.002
	65.50	0.22322	0.00458	0.22581	0.997	1.001	1.004	1.000	1.000
	75.00	0.20815	0.00458	0.21139	0.997	1.001	1.008	1.000	1.000
0.35	32.50	0.17975	0.00302	0.18002	0.998	1.003	0.998	1.000	1.005
	37.50	0.17028	0.00220	0.17061	0.998	1.003	1.002	1.000	1.003
	43.00	0.17086	0.00216	0.17128	0.998	1.003	1.005	1.000	1.002
	49.50	0.16730	0.00215	0.16784	0.998	1.003	1.003	1.000	1.002
	57.00	0.16606	0.00226	0.16677	0.998	1.003	1.006	1.000	1.002
	65.50	0.16045	0.00240	0.16136	0.998	1.003	0.998	1.000	1.001
	75.00	0.15978	0.00301	0.16098	0.998	1.003	1.001	1.000	1.000
	86.00	0.16018	0.00314	0.16179	0.998	1.003	1.007	1.000	1.000
	99.00	0.14935	0.00337	0.15136	0.998	1.003	1.003	1.000	1.000

Table 5: $F_2(x,Q^2)$ at 200 GeV beam energy (continued)

x	$Q^2\ (GeV^2)$	F_2^0	ΔF_2	F_2^{QCD}	f_b	f_s	f_r	f_d	f_n
0.45	32.50	0.10618	0.00273	0.10628	1.003	1.011	1.007	1.000	1.005
	37.50	0.10392	0.00292	0.10404	1.002	1.010	1.003	1.000	1.005
	43.00	0.10567	0.00190	0.10582	1.002	1.009	1.005	1.000	1.002
	49.50	0.10340	0.00189	0.10359	1.001	1.008	1.001	1.000	1.002
	57.00	0.10321	0.00195	0.10345	1.000	1.007	0.996	1.000	1.002
	65.50	0.10038	0.00205	0.10068	1.000	1.006	1.004	1.000	1.002
	75.00	0.09919	0.00258	0.09958	0.999	1.006	1.002	1.000	1.000
	86.00	0.09492	0.00261	0.09540	0.999	1.005	1.006	1.000	1.000
	99.00	0.09065	0.00270	0.09126	0.998	1.005	1.000	1.000	1.000
	115.50	0.09187	0.00272	0.09271	0.998	1.005	1.004	1.000	1.000
0.55	32.50	0.05383	0.00192	0.05387	1.014	1.027	1.025	1.000	1.005
	37.50	0.05319	0.00214	0.05323	1.011	1.023	1.020	1.000	1.005
	43.00	0.05346	0.00132	0.05352	1.009	1.021	1.014	1.000	1.002
	49.50	0.05282	0.00135	0.05289	1.007	1.018	1.013	1.000	1.002
	57.00	0.05373	0.00147	0.05382	1.005	1.016	1.007	1.000	1.002
	65.50	0.05221	0.00154	0.05231	1.004	1.014	1.002	1.000	1.001
	75.00	0.05218	0.00169	0.05231	1.003	1.013	1.002	1.000	1.001
	86.00	0.04913	0.00198	0.04929	1.002	1.011	1.005	1.000	1.000
	99.00	0.05086	0.00213	0.05107	1.001	1.010	1.001	1.000	1.000
	115.50	0.04983	0.00214	0.05010	1.000	1.009	1.000	1.000	1.000
	137.50	0.04556	0.00213	0.04591	0.999	1.008	1.004	1.000	1.000
0.65	32.50	0.02538	0.00115	0.02539	1.034	1.056	1.064	1.000	1.005
	37.50	0.02531	0.00128	0.02533	1.029	1.048	1.060	1.000	1.005
	43.00	0.02316	0.00074	0.02318	1.024	1.042	1.050	1.000	1.001
	49.50	0.02468	0.00082	0.02471	1.020	1.037	1.044	1.000	1.001
	57.00	0.02318	0.00085	0.02321	1.016	1.032	1.033	1.000	1.001
	65.50	0.02269	0.00094	0.02272	1.013	1.028	1.023	1.000	1.001
	75.00	0.02195	0.00103	0.02199	1.010	1.025	1.014	1.000	1.001
	86.00	0.02052	0.00123	0.02057	1.008	1.022	1.011	1.000	1.000
	99.00	0.02144	0.00138	0.02150	1.005	1.019	1.012	1.000	1.000
	115.50	0.01997	0.00135	0.02005	1.003	1.017	1.008	1.000	1.000
	137.50	0.01944	0.00146	0.01954	1.002	1.015	1.005	1.000	1.000
0.75	43.00	0.00934	0.00046	0.00935	1.054	1.087	1.135	1.000	1.000
	49.50	0.00935	0.00049	0.00936	1.045	1.076	1.120	1.000	1.000
	57.00	0.00830	0.00053	0.00831	1.038	1.066	1.111	1.000	1.000
	65.50	0.00764	0.00055	0.00765	1.031	1.058	1.100	1.000	1.000
	75.00	0.00803	0.00063	0.00804	1.025	1.050	1.092	1.000	1.000
	86.00	0.00720	0.00064	0.00721	1.020	1.044	1.077	1.000	1.000
	99.00	0.00857	0.00081	0.00859	1.016	1.039	1.068	1.000	1.000
	115.50	0.00673	0.00074	0.00675	1.012	1.033	1.055	1.000	1.000
	137.50	0.00661	0.00081	0.00664	1.008	1.029	1.042	1.000	1.000

Table 6: $F_2(x,Q^2)$ at 280 GeV beam energy

x	$Q^2\,(GeV^2)$	F_2^0	ΔF_2	F_2^{QCD}	f_b	f_s	f_r	f_d	f_n
0.10	32.50	0.36758	0.00737	0.37969	0.997	0.999	1.008	1.005	1.010
	37.50	0.35901	0.00803	0.37547	0.997	1.000	1.004	1.005	1.010
0.14	37.50	0.32900	0.00825	0.33370	0.996	0.999	1.005	1.000	1.010
	43.00	0.32609	0.00818	0.33244	0.997	0.999	1.004	1.000	1.010
	49.50	0.32622	0.00861	0.33497	0.997	1.000	1.004	1.000	1.010
	57.00	0.31362	0.00991	0.32518	0.997	1.000	1.004	1.000	1.010
0.18	37.50	0.29865	0.00862	0.30046	0.996	0.999	0.998	1.000	1.010
	43.00	0.31101	0.00875	0.31355	0.996	0.999	0.999	1.000	1.010
	49.50	0.31237	0.00922	0.31585	0.997	1.000	1.002	1.000	1.010
	57.00	0.28775	0.00632	0.29215	0.997	1.000	1.002	1.000	1.004
	65.50	0.29090	0.00671	0.29697	0.997	1.000	1.003	1.000	1.004
0.225	37.50	0.25886	0.00788	0.25963	0.996	0.999	0.996	1.000	1.010
	43.00	0.26717	0.00791	0.26822	0.996	0.999	1.004	1.000	1.010
	49.50	0.27703	0.00827	0.27849	0.996	1.000	1.001	1.000	1.010
	57.00	0.25610	0.00582	0.25793	0.997	1.000	1.001	1.000	1.004
	65.50	0.24968	0.00597	0.25211	0.997	1.000	0.998	1.000	1.004
	75.00	0.25033	0.00645	0.25361	0.997	1.001	1.000	1.000	1.003
	86.00	0.24686	0.00699	0.25124	0.997	1.001	1.003	1.000	1.002
0.275	37.50	0.21158	0.00795	0.21193	0.996	1.000	0.997	1.000	1.010
	43.00	0.23148	0.00821	0.23198	0.997	1.000	1.000	1.000	1.010
	49.50	0.22144	0.00813	0.22207	0.997	1.001	0.997	1.000	1.010
	57.00	0.21174	0.00570	0.21255	0.997	1.001	0.994	1.000	1.004
	65.50	0.22404	0.00622	0.22518	0.997	1.001	1.004	1.000	1.004
	75.00	0.20388	0.00614	0.20527	0.997	1.001	1.004	1.000	1.004
	86.00	0.21105	0.00652	0.21299	0.997	1.001	1.000	1.000	1.003
	99.00	0.21380	0.00863	0.21647	0.997	1.001	0.998	1.000	1.000
	115.50	0.19842	0.00918	0.20187	0.997	1.002	0.998	1.000	1.000
0.35	43.00	0.17498	0.00592	0.17518	0.998	1.004	0.994	1.000	1.010
	49.50	0.17194	0.00581	0.17219	0.998	1.003	0.997	1.000	1.010
	57.00	0.16210	0.00398	0.16241	0.998	1.003	0.994	1.000	1.004
	65.50	0.16531	0.00420	0.16573	0.998	1.003	0.995	1.000	1.004
	75.00	0.15851	0.00426	0.15904	0.998	1.003	0.997	1.000	1.004
	86.00	0.15873	0.00439	0.15943	0.998	1.003	0.994	1.000	1.004
	99.00	0.15282	0.00459	0.15372	0.998	1.003	0.995	1.000	1.003
	115.50	0.15741	0.00572	0.15870	0.998	1.003	0.998	1.000	1.000
	137.50	0.14745	0.00582	0.14921	0.998	1.003	0.998	1.000	1.000

Table 6: $F_2(x,Q^2)$ at 280 GeV beam energy (continued)

x	$Q^2\,(GeV^2)$	F_2^0	ΔF_2	F_2^{QCD}	f_b	f_s	f_r	f_d	f_n
0.45	43.00	0.09549	0.00521	0.09555	1.004	1.012	0.987	1.000	1.010
	49.50	0.10062	0.00520	0.10071	1.003	1.011	0.987	1.000	1.010
	57.00	0.10240	0.00368	0.10251	1.002	1.010	0.993	1.000	1.004
	65.50	0.09812	0.00366	0.09825	1.001	1.008	0.995	1.000	1.004
	75.00	0.09646	0.00379	0.09663	1.000	1.008	0.998	1.000	1.004
	86.00	0.09645	0.00389	0.09667	1.000	1.007	0.995	1.000	1.004
	99.00	0.09914	0.00413	0.09943	0.999	1.006	0.998	1.000	1.003
	115.50	0.09543	0.00412	0.09581	0.999	1.006	0.995	1.000	1.002
	137.50	0.08773	0.00485	0.08823	0.998	1.005	0.999	1.000	1.000
	175.00	0.08977	0.00460	0.09061	0.998	1.005	0.998	1.000	1.000
0.55	43.00	0.05248	0.00393	0.05251	1.015	1.028	0.994	1.000	1.010
	49.50	0.05631	0.00429	0.05634	1.013	1.025	0.993	1.000	1.010
	57.00	0.05488	0.00272	0.05492	1.010	1.022	0.995	1.000	1.004
	65.50	0.05046	0.00272	0.05051	1.008	1.019	0.995	1.000	1.004
	75.00	0.05662	0.00311	0.05669	1.006	1.017	0.999	1.000	1.004
	86.00	0.04721	0.00282	0.04728	1.005	1.015	1.000	1.000	1.004
	99.00	0.04941	0.00312	0.04950	1.003	1.013	1.001	1.000	1.003
	115.50	0.04626	0.00305	0.04637	1.002	1.012	0.999	1.000	1.002
	137.50	0.04294	0.00365	0.04308	1.001	1.010	0.998	1.000	1.010
	175.00	0.03930	0.00312	0.03951	0.999	1.009	0.995	1.000	1.000
	230.00	0.04154	0.00459	0.04192	0.998	1.007	0.995	1.000	1.000
0.65	49.50	0.02536	0.00247	0.02537	1.031	1.052	1.039	1.000	1.010
	57.00	0.02487	0.00167	0.02488	1.026	1.045	1.030	1.000	1.004
	65.50	0.02242	0.00166	0.02244	1.022	1.040	1.019	1.000	1.004
	75.00	0.02378	0.00182	0.02380	1.018	1.035	1.014	1.000	1.003
	86.00	0.02280	0.00191	0.02282	1.014	1.031	1.011	1.000	1.002
	99.00	0.02297	0.00205	0.02300	1.011	1.027	1.008	1.000	1.002
	115.50	0.01986	0.00192	0.01989	1.008	1.023	1.008	1.000	1.001
	137.50	0.02027	0.00250	0.02032	1.006	1.020	1.007	1.000	1.000
	175.00	0.01814	0.00238	0.01820	1.003	1.016	1.009	1.000	1.000
	230.00	0.01605	0.00263	0.01614	1.000	1.013	1.008	1.000	1.000
0.75	57.00	0.00911	0.00106	0.00911	1.059	1.093	1.149	1.000	1.000
	65.50	0.00909	0.00107	0.00910	1.049	1.081	1.130	1.000	1.000
	75.00	0.00786	0.00105	0.00787	1.041	1.071	1.108	1.000	1.000
	86.00	0.00902	0.00127	0.00903	1.034	1.062	1.090	1.000	1.000
	99.00	0.00807	0.00124	0.00808	1.028	1.054	1.062	1.000	1.000
	115.50	0.00614	0.00120	0.00615	1.022	1.047	1.057	1.000	1.000
	137.50	0.00564	0.00122	0.00565	1.016	1.039	1.046	1.000	1.000
	175.00	0.00541	0.00116	0.00542	1.010	1.031	1.040	1.000	1.000
	230.00	0.00639	0.00172	0.00642	1.005	1.025	1.022	1.000	1.000

Figure Captions

Fig. 1: $R=\sigma_L/\sigma_T$ measured in this experiment as a function of x. Inner error bars are statistical only, outer error bars are statistical and systematic errors combined linearly. The systematic errors are dominated by the relative normalization uncertainty between data taken at different beam energies and are thus strongly correlated. The solid line is the next-to-leading order QCD prediction using $\Lambda_{\overline{MS}}$ = 220 MeV and a gluon distribution $xG(x,Q_0^2)=4.5(1-x)^8$ at Q_0^2 = 5 GeV^2 [2].

Fig. 2: The deuteron structure function $F_2(x,Q^2)$ measured at the three beam energies 120, 200 and 280 GeV, using $R=R_{QCD}$. At x < 0.275, $F_2(x,Q^2)$ has been multiplied by the factors shown in the figure. Only statistical errors are shown.

Fig. 3: The structure function $F_2(x,Q^2)$ from this experiment for all beam energies combined, using $R=R_{QCD}$. Also shown are data from the EMC [12] and SLAC [13] experiments. Where necessary, the EMC data were interpolated to the x bins of this experiment at each value of Q^2 using a third order polynomial. The relative normalizations between the experiments have not been adjusted; the normalization uncertainties are 3%, 5% and 2% for the BCDMS, EMC and SLAC data, respectively. At $x \leq 0.225$, all data have been multiplied by the factors indicated in the figure. The error bars are statistical and systematic errors combined in quadrature and are thus partially correlated.

Fig. 4: (a) The logarithmic derivatives $d\ln F_2(x,Q^2)/d\ln Q^2$ observed in this experiment, averaged over Q^2, for Q^2 > 20 GeV^2 and $x \geq 0.275$. The inner error bars are statistical, the outer error bars show statistical and systematic errors added linearly. The systematic errors are strongly correlated. The lines show nonsinglet QCD predictions for $\Lambda_{\overline{MS}}$ = 230 MeV and for two other values of Λ.

(b) The same as (a) but for the full x range of the data. The line shows a singlet QCD prediction for $\Lambda_{\overline{MS}}$ = 250 MeV, assuming a gluon momentum distribution

$xG(x,Q_0^2)=4.5(1-x)^8$ at Q_0^2 = 5 GeV^2 [2]. The QCD prediction fits the data with a χ_S^2/DOF = 19.0/10. Only statistical errors are shown.

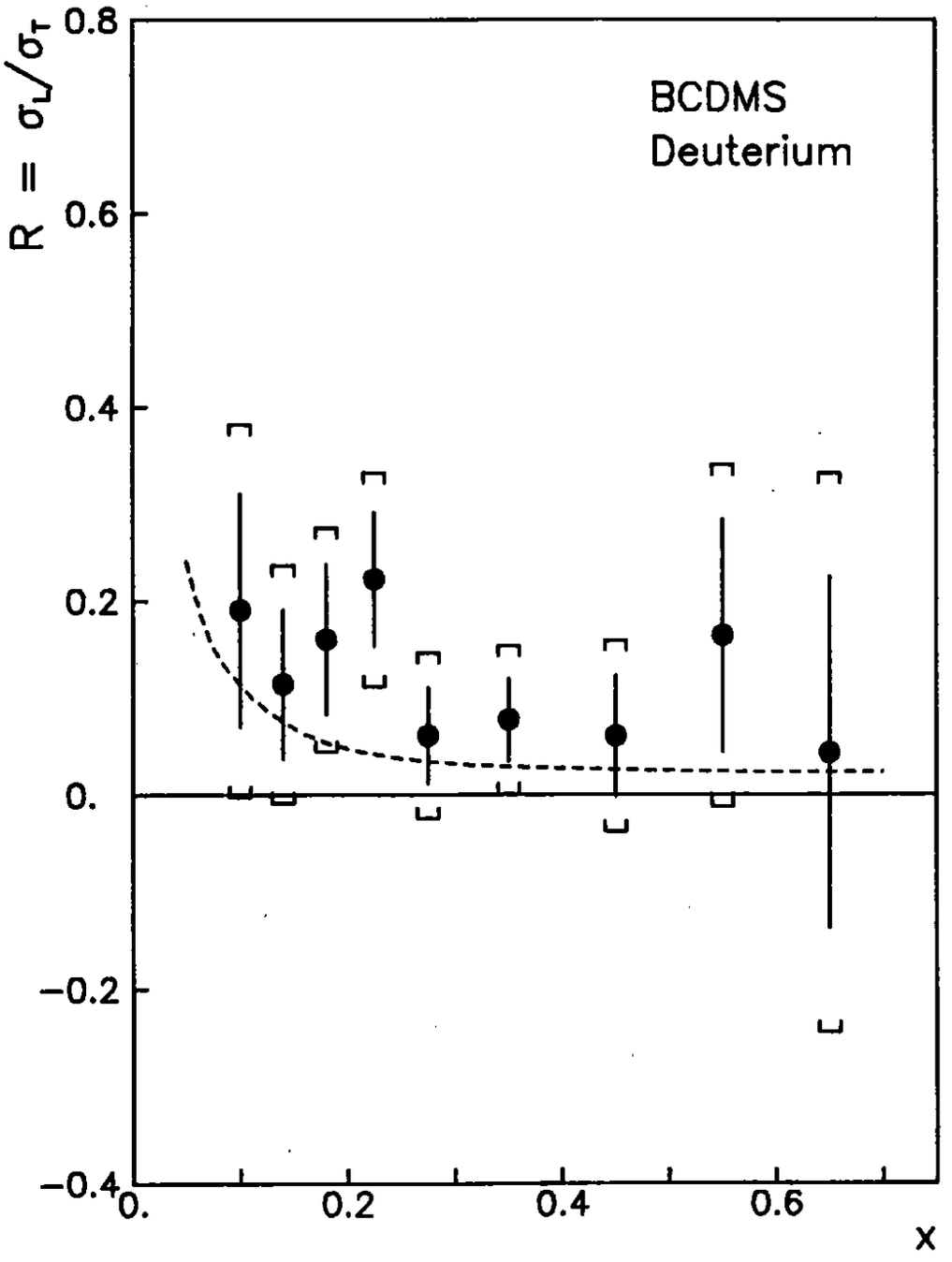

FIG. 1

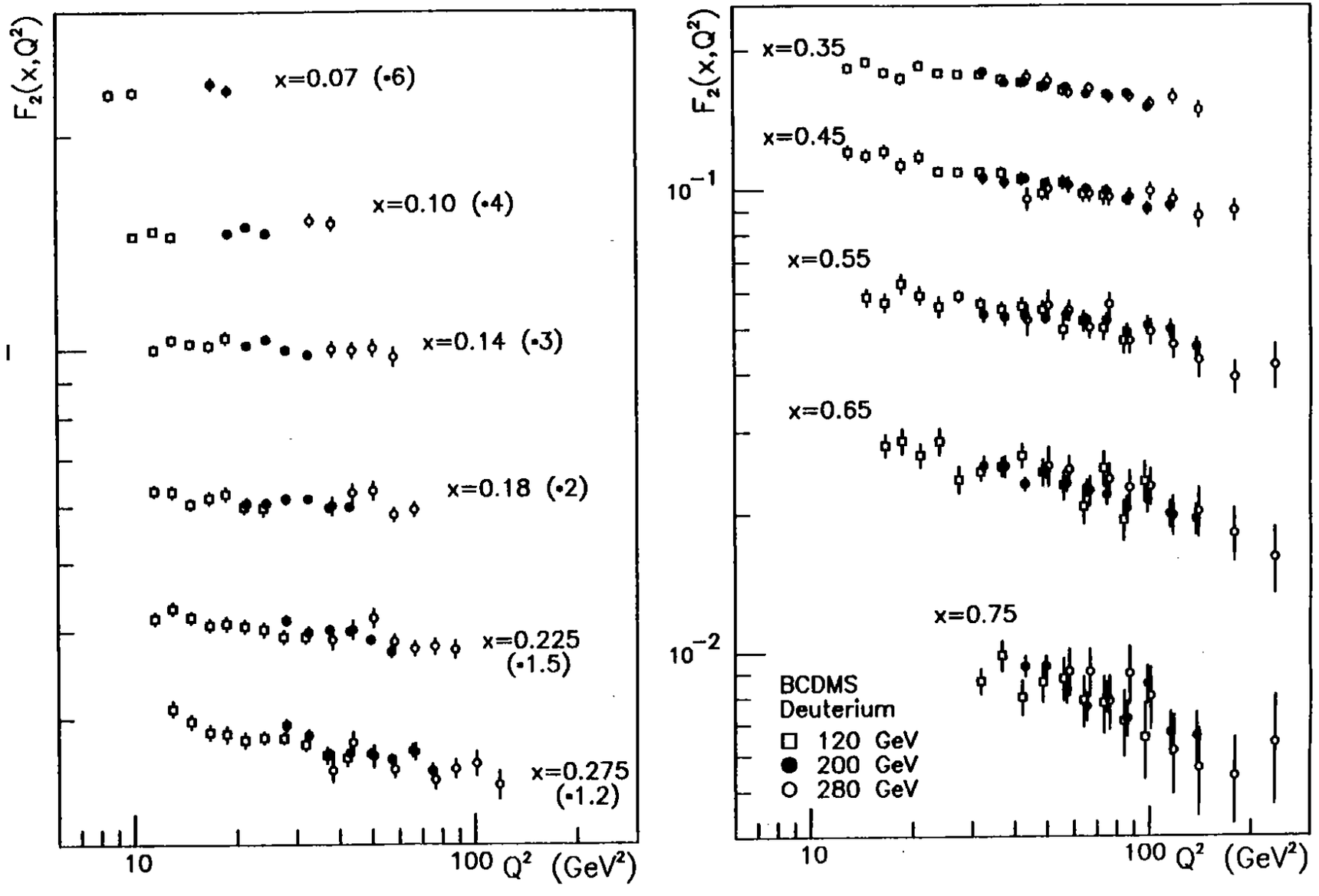
$F_2(x,Q^2)$
x=0.07 (•6)
x=0.10 (•4)
x=0.14 (•3)
x=0.18 (•2)
x=0.225 (•1.5)
x=0.275 (•1.2)
10
100 Q^2 (GeV^2)
$F_2(x,Q^2)$
x=0.35
x=0.45
x=0.55
x=0.65
x=0.75
10^{-1}
10^{-2}
BCDMS
Deuterium
120 GeV
200 GeV
280 GeV
10
100 Q^2 (GeV^2)

FIG. 2

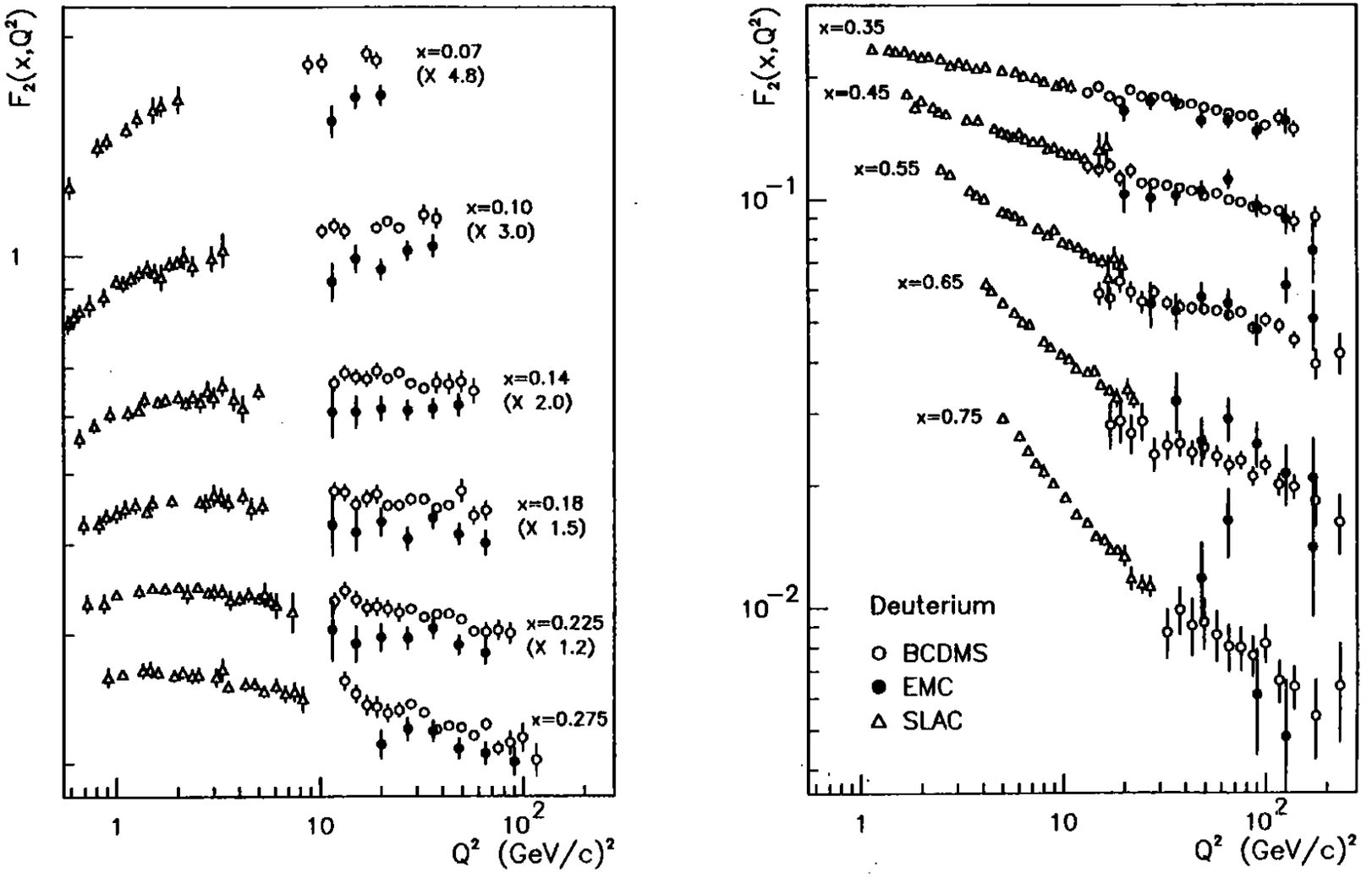
$F_2(x,Q^2)$
x=0.07
(X 4.8)
x=0.10
(X 3.0)
x=0.14
(X 2.0)
x=0.18
(X 1.5)
x=0.225
(X 1.2)
x=0.275
1
1
10
10^2
Q^2 (GeV/c)^2
$F_2(x,Q^2)$
x=0.35
x=0.45
x=0.55
x=0.65
x=0.75
10^{-1}
10^{-2}
Deuterium
BCDMS
EMC
SLAC
1
10
10^2
Q^2 (GeV/c)^2

FIG. 3

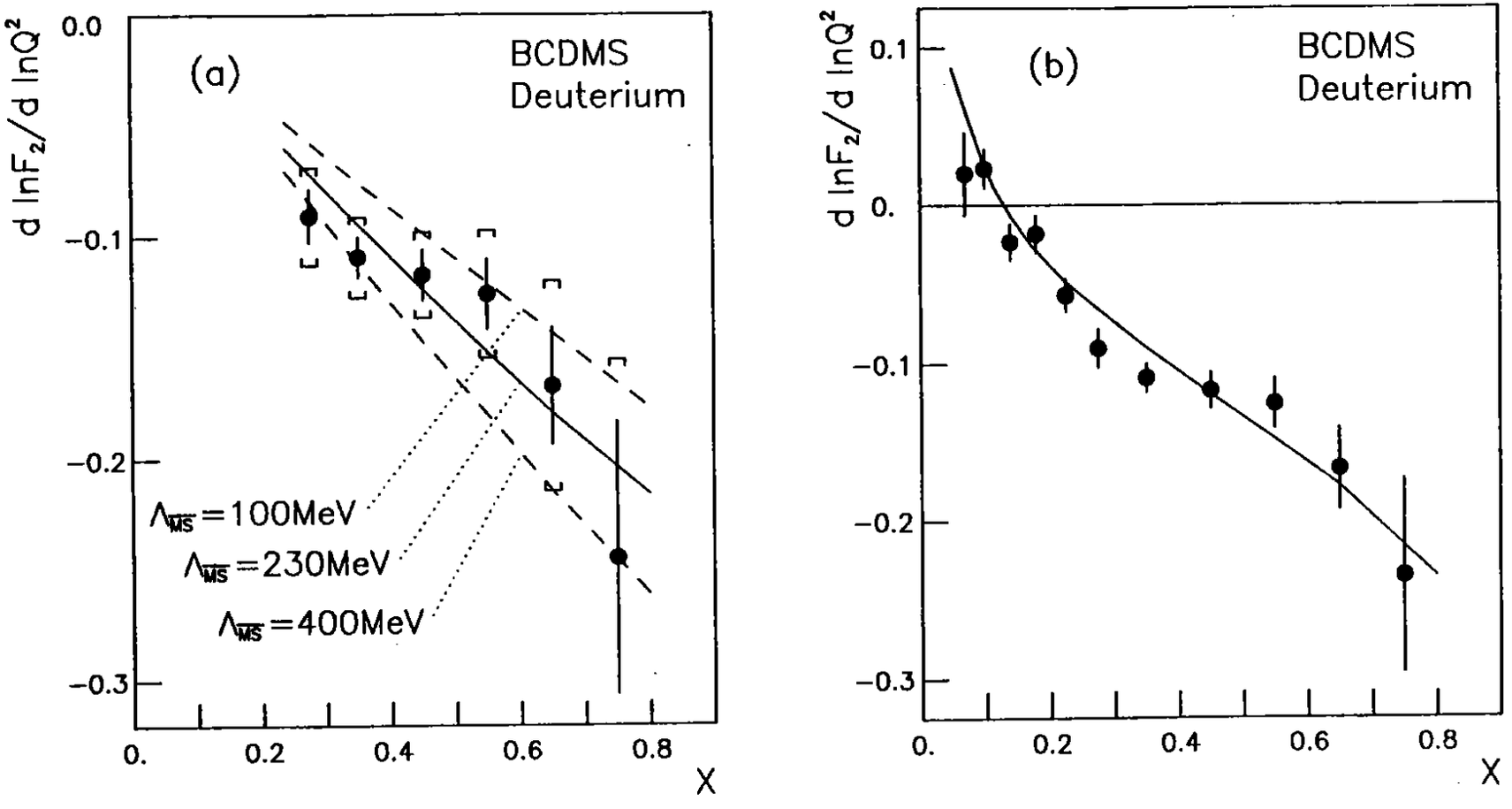
(a)
BCDMS
Deuterium
d lnF2/d lnQ2
0.0
−0.1
−0.2
−0.3
ΛMS=100MeV
ΛMS=230MeV
ΛMS=400MeV
0.
0.2
0.4
0.6
0.8
X
(b)
BCDMS
Deuterium
d lnF2/d lnQ2
0.1
0.
−0.1
−0.2
−0.3
0.
0.2
0.4
0.6
0.8
X

FIG. 4